REPORT DOCUMENTATION PAGE

Form Approved OMB No. 0704-0188

1. REPORT DATE *(DD-MM-YYYY)*
28-07-2005

2. REPORT TYPE
Final Report

3. DATES COVERED *(From – To)*
1 May 2004 - 01-May-05

4. TITLE AND SUBTITLE
AC Loss Minimisation in High Temperature Superconductors

5a. CONTRACT NUMBER
FA8655-04-1-3033

5b. GRANT NUMBER

5c. PROGRAM ELEMENT NUMBER

6. AUTHOR(S)
Professor Archie M Campbell

5d. PROJECT NUMBER

5d. TASK NUMBER

5e. WORK UNIT NUMBER

7. PERFORMING ORGANIZATION NAME(S) AND ADDRESS(ES)
University of Cambridge
West Cambridge Site
Madingley Rd
Cambridge CB3 OHE
United Kingdom

8. PERFORMING ORGANIZATION REPORT NUMBER
N/A

9. SPONSORING/MONITORING AGENCY NAME(S) AND ADDRESS(ES)
EOARD
PSC 821 BOX 14
FPO 09421-0014

10. SPONSOR/MONITOR'S ACRONYM(S)

11. SPONSOR/MONITOR'S REPORT NUMBER(S)
Grant 04-3033

12. DISTRIBUTION/AVAILABILITY STATEMENT

Approved for public release; distribution is unlimited.

13. SUPPLEMENTARY NOTES

14. ABSTRACT

This report results from a contract tasking University of Cambridge as follows: The contractor will investigate:
1) AC losses of appropriate Yttrium Barium Copper Oxide (YBCO) samples with strong potential for minimizing losses at high frequencies and magnetic fields with the existing equipment. Measurements will be made using copper split solenoid apparatus, which can produce 0.3 tesla (peak) at 50Hz.
2) The effect of filament width and grain size on losses. The loss should be inversely proportional to the width so fine filaments are required. However the inevitable presence of low angle grain boundaries means that if the width is less than that of a few grains there may not be a high current percolation path along the whole conductor. The best compromise between the two conflicting criteria will be determined.
3) Thermal stability of conductors.
4) Coupling losses at high frequencies and long conductor lengths.
5) Model conductor losses and stability in a complete winding.
5) Superconducting filaments isolated from the substrate will be investigated and techniques for reducing losses will be evaluated.
6) Transport losses in long length conductors will be measured using helical windings.

15. SUBJECT TERMS
EOARD, Aircraft Subsystem, Power, Superconductivity

16. SECURITY CLASSIFICATION OF: a. REPORT	b. ABSTRACT	c. THIS PAGE	17. LIMITATION OF ABSTRACT	18, NUMBER OF PAGES	19a. NAME OF RESPONSIBLE PERSON
UNCLAS	UNCLAS	UNCLAS	UL	18	MICHAEL KJ MILLIGAN, Lt Col, USAF
					19b. TELEPHONE NUMBER *(Include area code)* +44 (0)20 7514 4955

Standard Form 298 (Rev. 8/98)
Prescribed by ANSI Std. Z39-18

Final Report on EOARD Contract No F61775-01-WE92z
1 October 2003-31 March 2005.
Extension to AC Loss Minimisation in High Temperature Superconductors

A.M.Campbell, M.Majoros and B.A.Glowacki.
IRC in Superconductivity, Madingley Road, Cambridge U.K.

1. Summary

During this time period of the contract the work proceeded simultaneously on thermal stability modelling, measuring ac losses and on upgrading the measuring system for frequencies up to 420 Hz. Software has been developed to model the quenching and current sharing process. When a voltage source was used the presence of defects led to current limiting effects. Using a current source caused significant overheating. AC losses in different samples (Rabits-monolayer, Rabits-20 filaments, Ibad-monolayer) as well as in the substrate have been measured up to 420 Hz in an applied magnetic field. AC losses in Rabits samples with different kinds of well defined inter-filament bridging, designed to aid current sharing between filaments, have also been measured and a method of bridging the filaments as a way of improving stability was assessed. Hall probe magnetometry of samples with interconnected filaments has been developed. DC current-voltage characteristics and transport ac losses have been measured on a Rabits sample CM1, which consisted of a monolayer and a striated (filamentary) part. These measurements have been performed at frequencies 40 Hz – 2 kHz. A degradation in I_c of about 40% due to the laser striation process has been found. The striated sample was much more stable than the monolayer sample. Transport ac losses were weakly frequency dependent up to 2 kHz, and mainly determined by the losses in the substrate and Ni layer up to currents of about 50% of I_c. Striation had no effect on normalized transport ac losses, which are basically hysteretic. Comparison of transport ac losses with in-field losses showed that the dominant loss contribution is the in-field loss. Software has been written to model the thermal stability of the conductors. However it needs more detailed material properties than we have at present so the conclusions on stability are essentially qualitative.

2. Results

2.1 AC loss measurements up to 420 Hz in monolayer samples, substrates and striated samples with no superconducting bridging between the filaments

Main conclusions:

1) At f=46.7 Hz – 93.9 Hz ac losses measured in December 2003 were the same seven months later so there has been no degradation. (The samples were kept in a dessicator).
2) AC losses in the substrate (with the top Ni layer removed) are low – about 1 order of magnitude lower than the ac losses in the Rabits 20 filament sample (with no superconducting bridging) (Fig. 1) These losses could be measured with a sufficient accuracy only at 420 Hz since they were too low at lower frequencies.
3) AC losses in the Rabits-20 filament sample (with no superconducting bridging) vary approximately as the square of the applied magnetic field (Fig. 2) and the energy loss depends linearly on frequency (Fig. 3). This behavior may be explained by electrical connections between YBCO filaments and the substrate in the grooves between the filaments due to laser ablation. During this process metals melt and may couple the YBCO filaments with the substrate so the measured losses are basically the coupling losses due to the substrate.
4) The AC loss per cycle in Rabits-monolayer and Ibad-monolayer samples are frequency independent (Fig. 4, Fig. 5), but a sudden ac loss increase was observed at 214 Hz in fields close to 100 mT. This increase is reproducible and appears only in these two samples which had rather high losses. We think that it is connected with heating of the sample in the sample holder. The full penetration field decreases (because J_c decreases), so ac losses in the YBCO film are lower and an additional loss in the Ag coating starts to be visible (this depends on the square of

the applied magnetic field – compare Fig. 4 and Fig. 5 at 214 Hz). At 420 Hz there is a tendency to see a similar effect, but the field amplitude is not high enough to see the onset of the loss in the Ag coating. This effect requires further study.

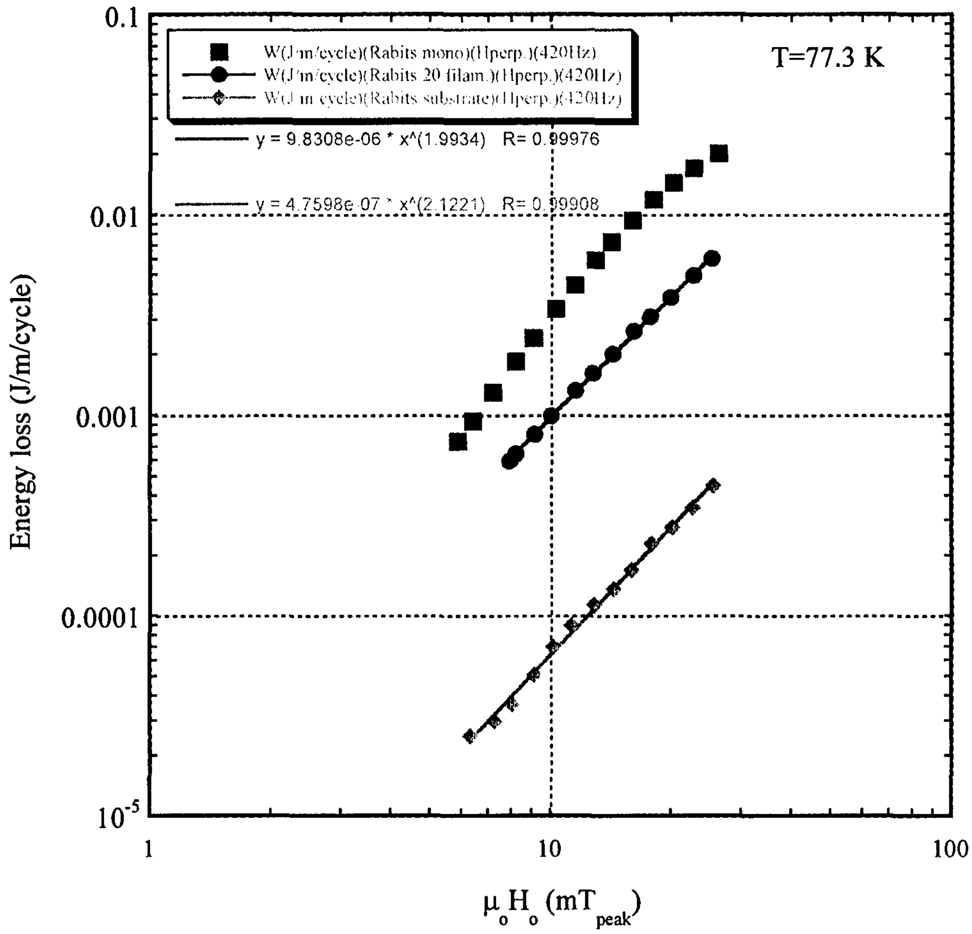

Fig. 1: Energy loss of a Rabits-monolayer sample, a Rabits-20 filament sample with no superconducting bridging between the filaments and of a Ni-5at%W substrate sample (with the top Ni layer removed), measured in an applied magnetic field perpendicular to the broader face of the samples at 420 Hz in a liquid nitrogen bath.

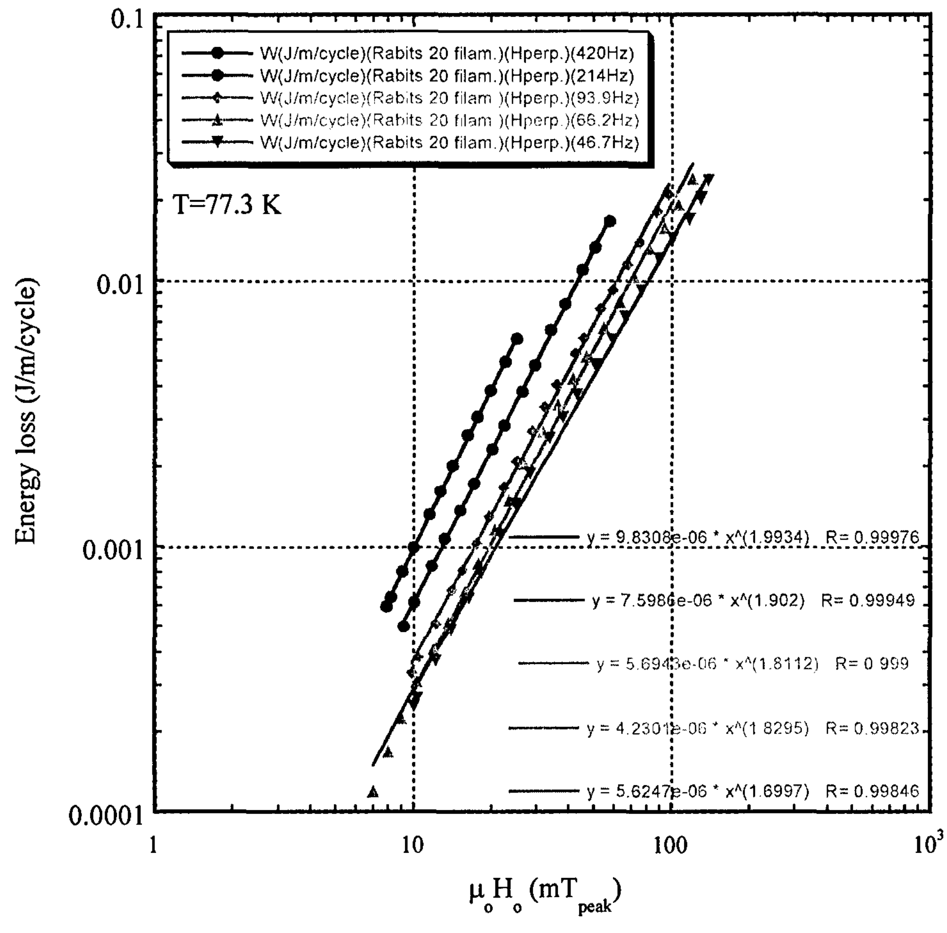

Fig. 2: Energy loss of a Rabits-20 filament sample with no superconducting bridging between the filaments, measured in an applied magnetic field perpendicular to the broader face of the sample at different frequencies in a liquid nitrogen bath

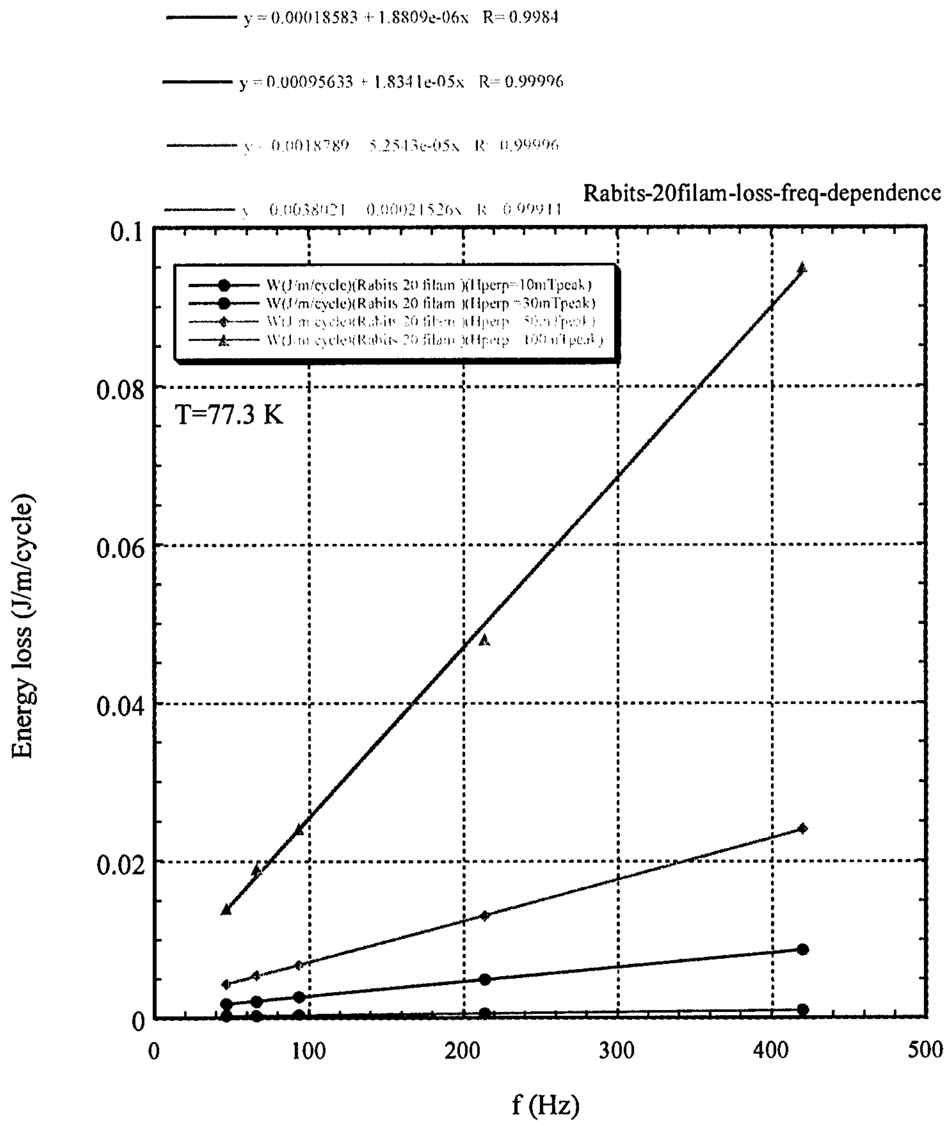

Fig. 3: Frequency dependence of the energy loss of a Rabits-20 filament sample, with no superconducting bridging between the filaments, at different magnetic fields applied perpendicularly to the broader face of the sample in a liquid nitrogen bath.

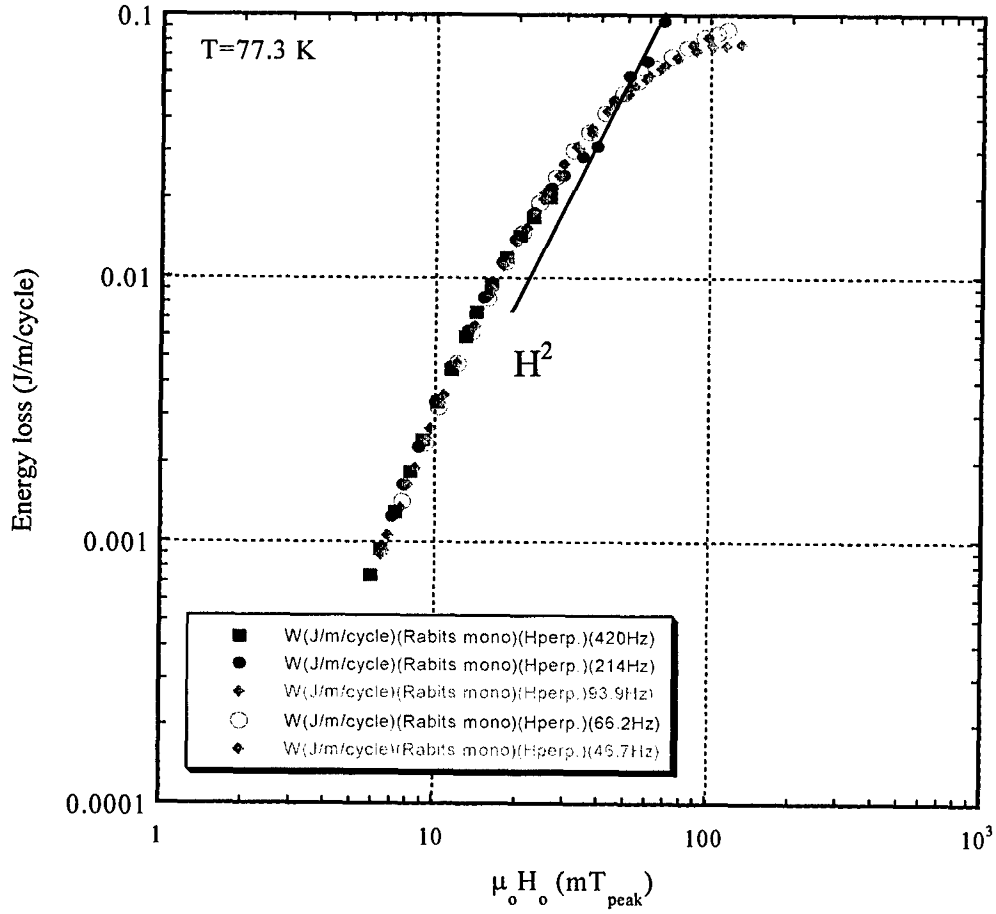

Fig. 4: Energy loss of a Rabits-monolayer sample measured in an applied magnetic field perpendicular to the broader face of the sample at different frequencies in liquid nitrogen bath.

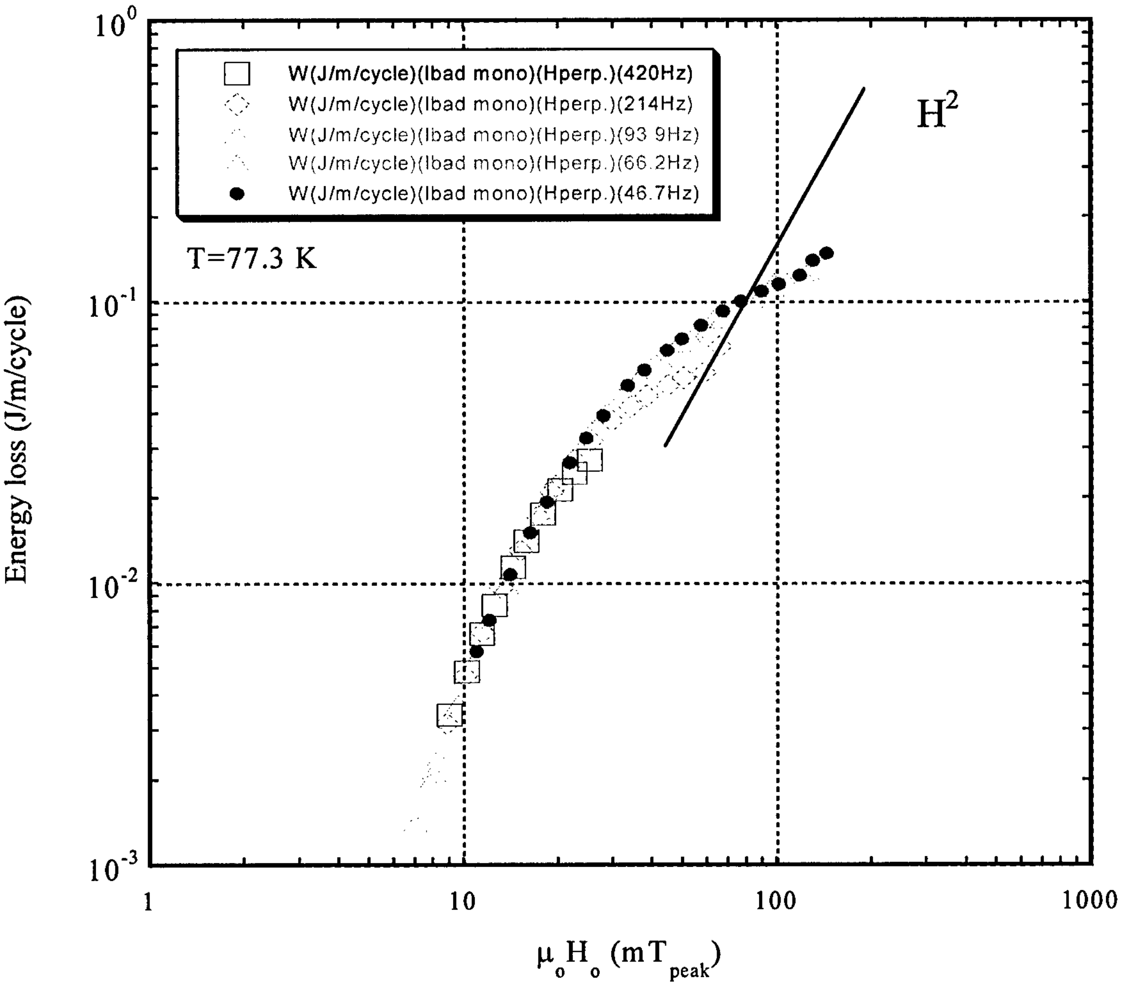

Fig. 5: Energy loss of an Ibad-monolayer sample measured in an applied magnetic field perpendicular to the broader face of the sample at different frequencies in a liquid nitrogen bath.

2.2 AC losses in samples with well defined superconducting filament bridging

Sample C5 Sample C6

Fig. 6: Striated tapes with interconnected filaments (20 filaments each). Sample C5 – interlocking cuts (3 segments per 1 cm), Sample C6 – alternating bridges (6 per 1 cm).

The geometry of the samples C5 and C6 with well defined superconducting bridges between the filaments is shown in Fig. 6. AC losses at different frequencies in a magnetic field applied perpendicularly to the face of the samples C0 (monolayer sample), C5 and C6 are shown in Fig. 7. The frequency dependence of the losses is quite weak and the losses of all the samples are basically hysteretic. They roughly follow H^3 and H^1 dependencies, in accordance with the critical state model with J_c independent of magnetic field.

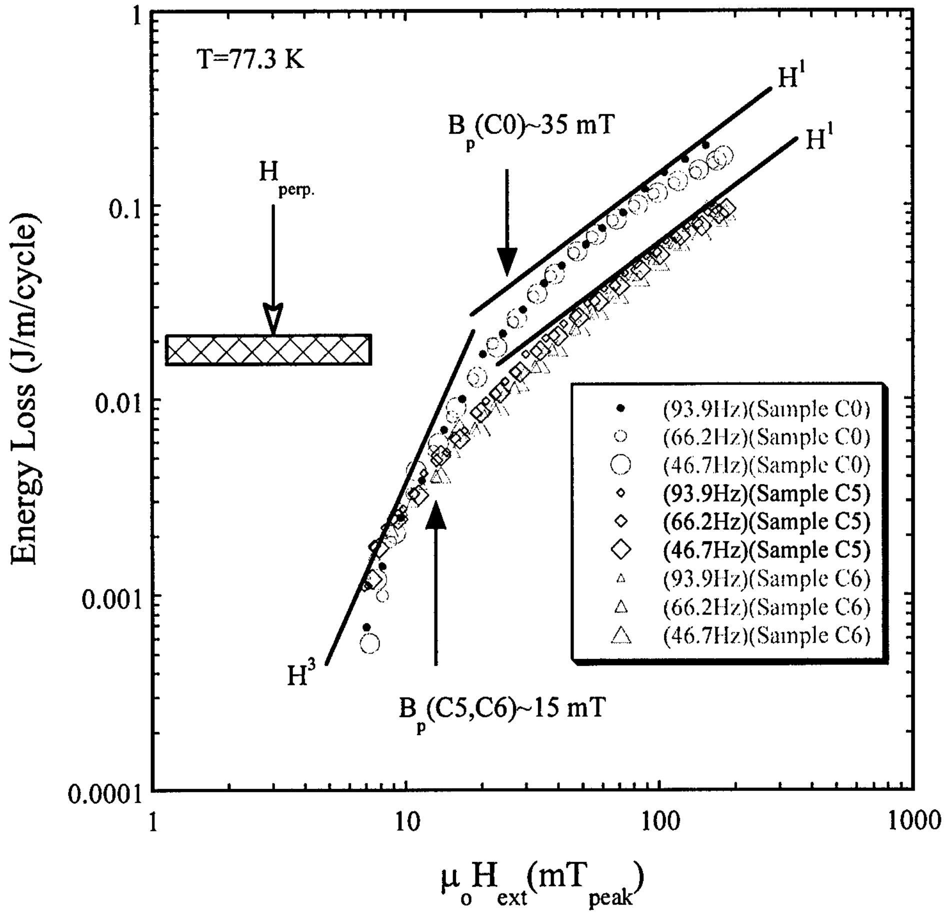

Fig. 7. AC losses of the samples C0 (monolayer sample), C5 and C6 in an applied magnetic field perpendicular to their broader face at different frequencies (B_p – estimates of full penetration fields of the corresponding samples).

Given the fact that the filaments are separated by insulating barriers and that the filament bridges are superconducting, ac losses of Sample C5 and C6 can be analyzed using an anisotropic critical state model for a multifilamentary medium. For an analysis of such a multifilamentary medium, the critical current density J_c characterizing the homogeneous material must be replaced by a current density $J_s=x_sJ_c$, where x_s is the relative amount of the superconducting component (filling factor). If we denote $J_{s||}=x_{s||}J_c$ the current density parallel to the filaments and $J_{s\perp}=x_{s\perp}J_c$ the current density perpendicular to the filaments (i.e. flowing across the bridges), then for both samples C5 and C6 we obtain $J_{s||}=0.8J_c$ and $J_{s\perp}=0.055J_c$ (because the YBCO film is isotropic – there is no difference between J_c along and across the YBCO film). This gives a geometrical anisotropy factor $\gamma=J_{s||}/J_{s\perp}=14.54$. For fields at full penetration we obtain $H_{p||}=J_{s||}w/2$ and $H_{p\perp}=J_{s\perp}l/2$, where w is the width and l the length of the sample. The ratio is $H_{p||}/H_{p\perp}=3.63$, which is comparable to the estimated experimental values in Fig. 7. This means that the field starts to penetrate from the ends of the samples. In the full penetration regime the field fully penetrates from the ends of the samples, while the penetration depth from the sides is only about 1.4 mm. The situation is schematically depicted in Fig. 8a. This should be compared with the monolayer sample C0, in which case the field fully penetrates from the sides, the penetration depth is equal to the half width of the sample, i.e. 5 mm; and because J_c is the same across the width of the sample, the same penetration depth (i.e. 5 mm) will be found at the ends of the sample. This situation is schematically shown in Fig. 8b.

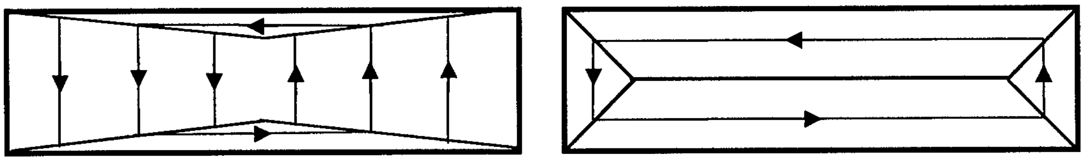

a) b)

Fig. 8. Screening currents in Samples C5, C6 (a) and in Sample C0 (monolayer sample) (b) at full penetration (schematic).

The simplest way to compare the ac losses of samples C0 and C5, C6 is to calculate saturation magnetization in the fully penetrated state M_s. Then the ac losses at fields $H_m >> H_p$ are directly proportional to M_s. We derived the following expression for M_s for samples C5, and C6 (anisotropic multifilamentary medium fully penetrated from its ends, Fig. 8a) assuming J_c=const.

$$M_{s(multi)} = -\frac{J_{s\perp} l}{4}\left[1-\frac{l}{3w}\frac{J_{s\perp}}{J_{s\parallel}}\right] \qquad 1$$

This should be compared with the corresponding result for a continuous isotropic medium fully penetrated from the sides, Fig. 8b (Sample C0)

$$M_{s(mono)} = -J_c\frac{w}{4}\left(1-\frac{w}{3l}\right) \qquad 2$$

Using the above expressions we obtained a value of 4.6 for the loss ratio defined as $M_{s(mono)}/M_{s(multi)}$ (The loss of Sample C0 divided by the loss of Sample C5 or C6). From experiment at fields ~200 mT we obtained a value of 2. The difference can be explained partially by the simplicity of the theoretical model used (valid for infinitely long orthorhombic samples) as well as by the fact, that the model considers that the coupling currents flow perpendicularly to the filaments. This is not the case for Samples C5 and C6, where at their ends the current must partially flow along the filaments in a "meandering" way (this can be deduced from the geometry of the samples in Fig. 6 as well as from modeling in Fig. 12 and Fig. 13), which causes additional losses. Also only the coupling losses due to currents between the filaments were considered in the model. In reality there is also a contribution to the losses due to currents which close within the filaments.

Although for the particular samples C0, C5 and C6 the ac loss reduction was only a factor of 2, it may be higher for longer samples at lengths and fields where the penetration depth at the ends is much smaller than the half-length of the sample. This justifies the use of filament bridging as a method of stabilization of multifilamentary coated conductors. However a compromise between the degree of stabilization and ac loss increase due to filament coupling must be made.

The problem is similar to that of using a protective normal layer (Ag) as a stabilizer. Although its influence on the ac losses of monolayer samples is negligible, most likely it will not be possible to use a continuous protective layer in the case of filamentary samples, when ac losses in YBCO will become significantly reduced.

2.3 Magnetic field profiles measured by Hall probe on a model sample C5 (containing only one interlocking cut - zipper)

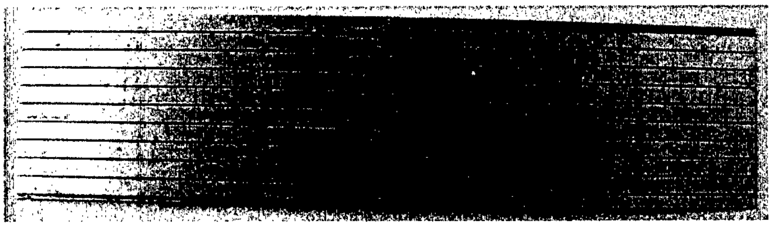

Fig. 9: Model sample C5 containing only 1 interlocking cut (zipper), 2 segments per 4 cm (number of strips: 10, width of a strip 1 mm, width of resistive barrier 70 μm).

Magnetic field profiles due to trapped currents in the sample have been measured. Fig. 10 shows the results above the central part of the model sample C5 containing only one interlocking cut of the filaments (see Fig. 9). The results show that the screening currents mostly close within the individual strips on each half of the sample (see numerical modeling results in Fig. 11).
On increasing the number of interlocking cuts the screening currents start to close at the ends of the sample (Fig. 12, Fig. 13). This situation is relevant to the case of Sample C5 (Fig. 6) containing multiple interlocking cuts (with 3 segments per 1 cm).

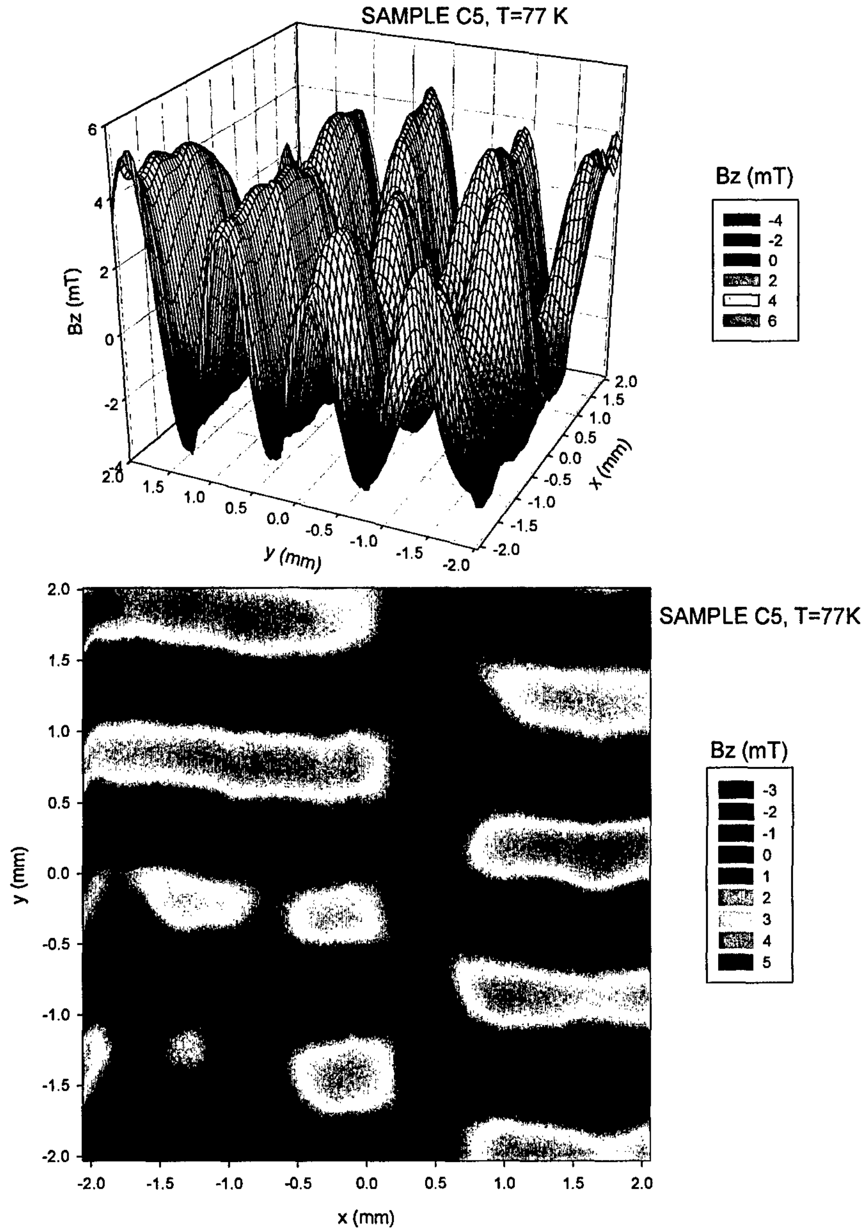

Fig. 10: Trapped magnetic field profiles of the model sample C5 containing only 1 interlocking cut (zipper) in its central part (Fig. 9) measured by a Hall probe at 77 K. Shown in the figure is the central part (zipper) of the sample.

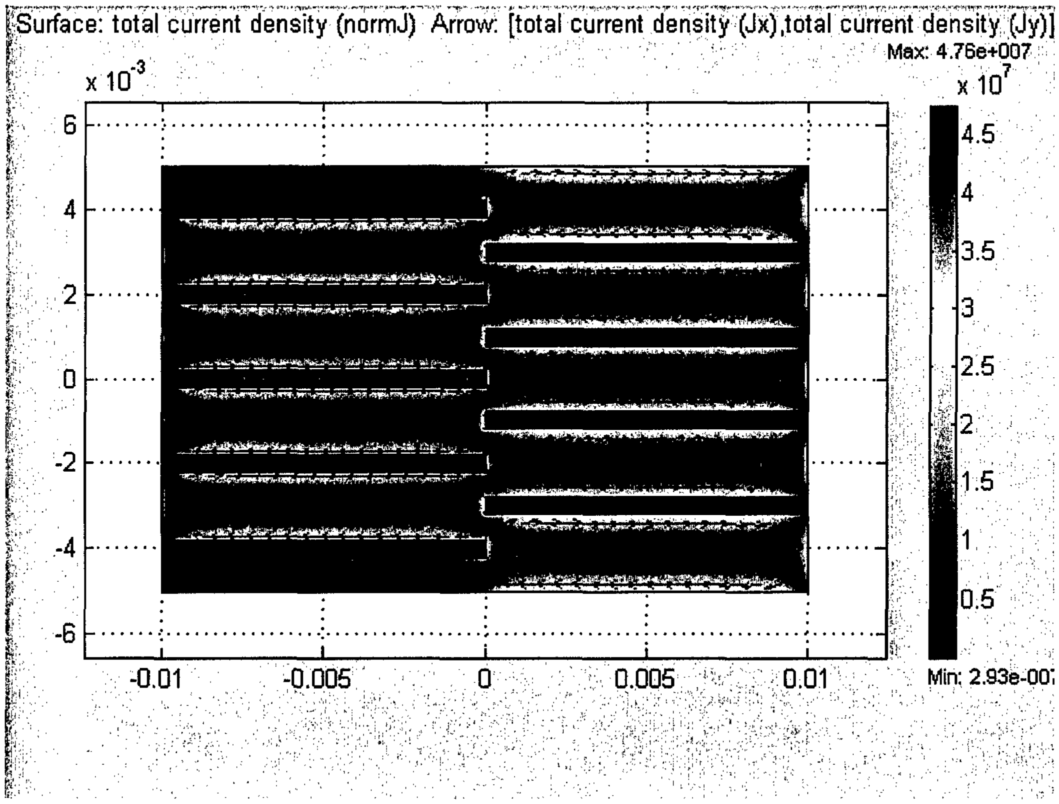

Fig. 11: Screening currents in the model sample C5 containing only 1 interlocking cut of the filaments (Fig. 9) – numerical modeling (compare with Fig. 10).

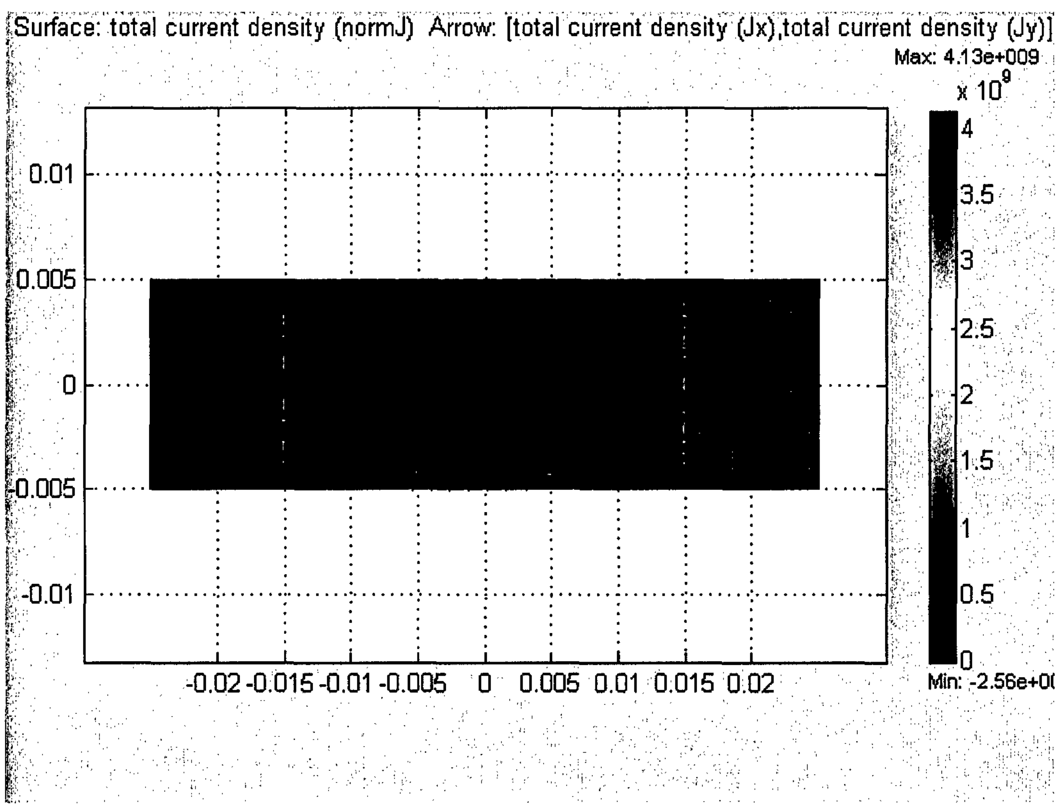

Fig. 12: Screening currents in a sample with 4 interlocking cuts – numerical modeling.

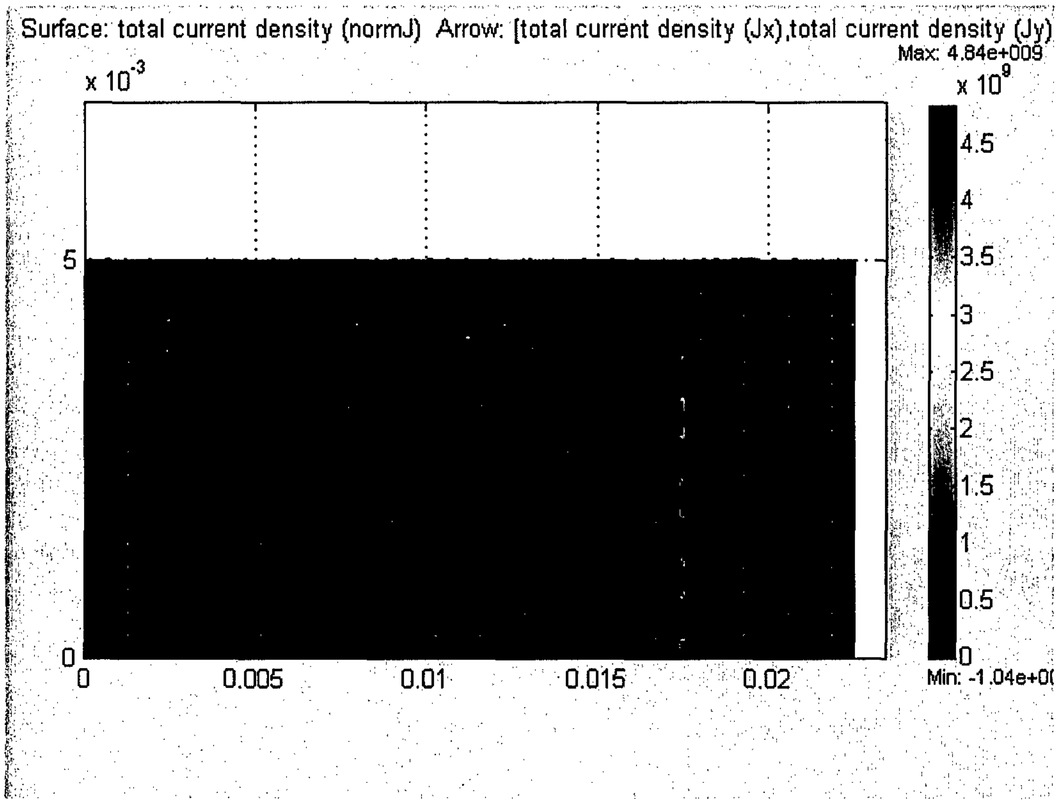

Fig. 13: Screening currents in a sample with 8 interlocking cuts – numerical modeling (only the 1st quadrant of the sample cross-section is shown).

2.4 DC current-voltage characteristics measurements

DC current-voltage characteristics and transport ac losses of Rabits sample CM1 have been measured. The sample consisted of 2 parts – a monolayer and a striated part. DC current-voltage characteristics have been measured in self-magnetic field at 77 K. The monolayer sample showed a significant degree of instability at $I<I_c$ (see Fig. 14, noisy regions below 200 A). In this respect the multifilamentary sample was much more stable (Fig. 15). The critical current of the monolayer sample I_c(mono) was 220 A, and the critical current of the filamentary sample I_c(filam) was 120 A, Both critical currents were determined at 1 μV/cm. The filling factor of the filamentary sample was 91.68%, so this sample should have a critical current of 201.69 A. The measured value of 120 A represents about 40% degradation, which is probably caused by the laser striation .

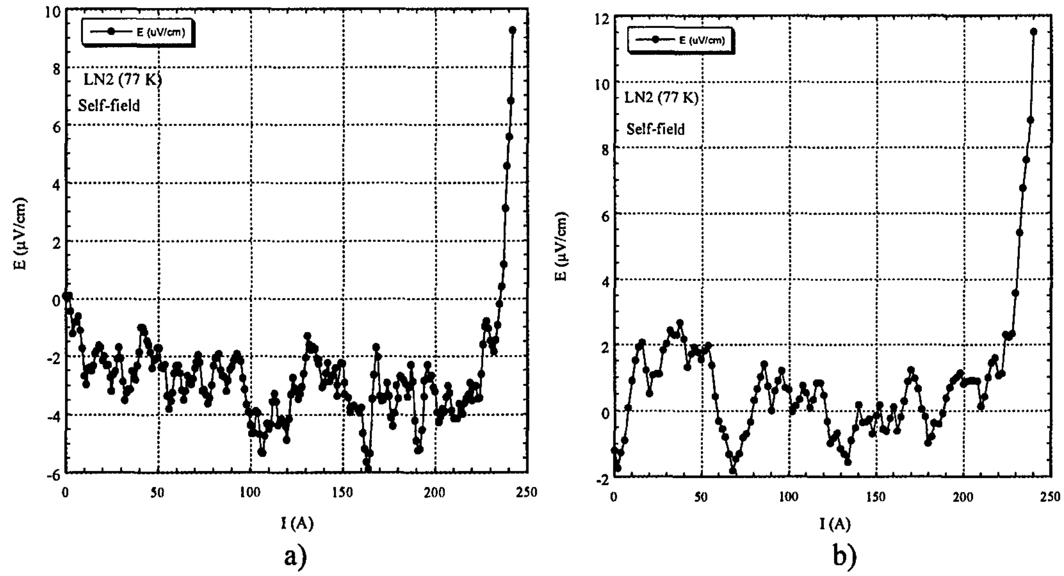

Fig. 14: DC current-voltage characteristic of Sample CM1 – monolayer part, $I_c(1\mu V/cm)$=220 A. a) first run, b) second run

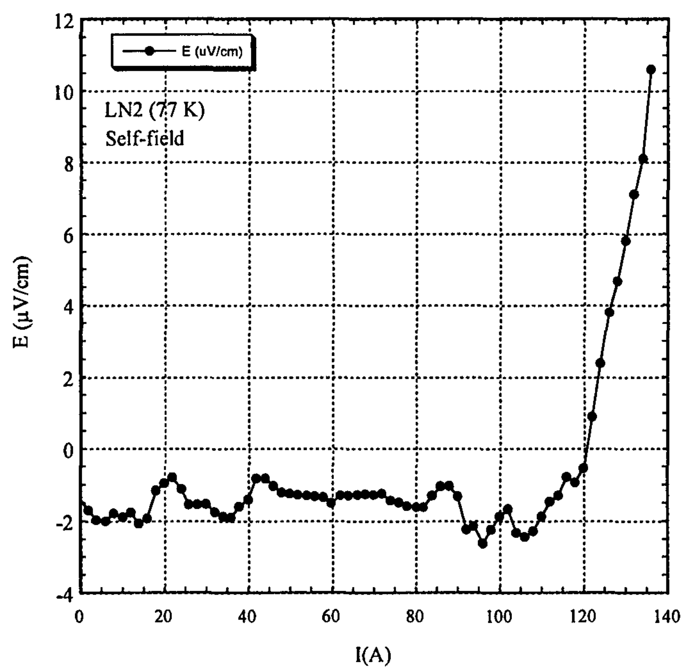

Fig. 15: DC current-voltage characteristic of Sample CM1 – filamentary part, $I_c(1\mu V/cm)$=120 A.

2.5 Transport AC losses in a monolayer and a striated sample at frequencies 40 Hz – 2 kHz

Transport ac losses have been measured in the frequency range 40 Hz – 2 kHz. The results for the monolayer sample are shown in Fig. 16. We obtained very interesting results. The energy loss per cycle is nearly independent of frequency and the losses are basically hysteretic. However their dependence does not follow I^3 as expected from the critical state model, but follows an I^2 dependence which is more characteristic of losses in a ferromagnetic material. Only at currents close to I_c do the measured losses follow the expected theoretical dependence for a superconducting cylinder of an elliptical cross-section, shown by the continuous blue line in Fig. 16. We believe that

this behavior is caused by magnetic losses in the substrate and in the thin Ni layer on top of it, due to self magnetic field generated by the transport current. Moreover, some instabilities started to be visible at frequencies of 960 Hz and 1920 Hz (see Fig. 16 pink and blue symbols, respectively). AC losses at 100 A, i.e. at about 50% of I_c, are about a factor of 2 higher than expected for a pure superconducting sample with no substrate. These results are important when considering the application of these tapes in power generators at frequencies greater than 1000 Hz.

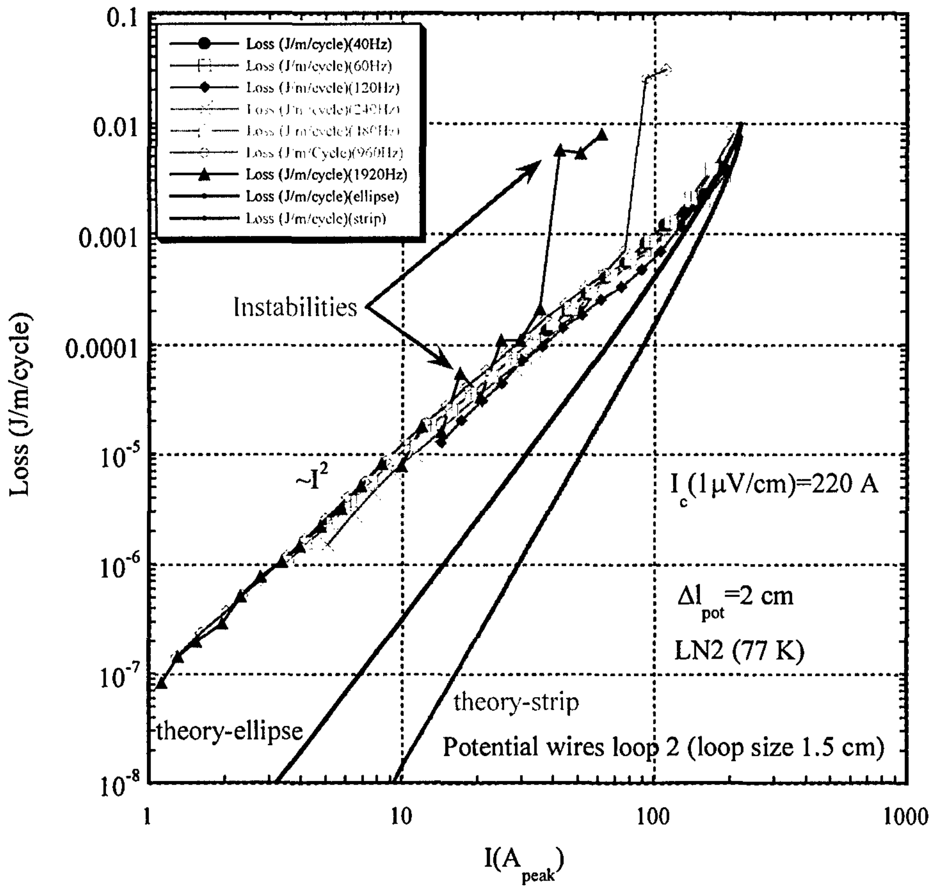

Fig. 16: Transport ac losses of Sample CM1 – monolayer part, $I_c(1\mu V/cm)$=220 A, measured in the frequency range 40 Hz – 2 kHz.

AC losses of the striated part of the sample CM1 are shown in Fig. 17. As for the monolayer sample the energy loss per cycle is nearly independent of frequency and the losses are basically hysteretic. They are due to the magnetization losses in the substrate structure caused by the self magnetic field generated by the transport current. Also in this sample some instabilities started to be visible at frequencies of 960 Hz and 1920 Hz (see Fig. 17 gray and pale pink symbols, respectively). AC losses of both samples are shown in a single graph in Fig. 18 and Fig. 19. Fig. 18 shows the losses of the samples plotted against the transport current, while Fig. 19 shows the normalized loss plotted against the normalized current. Both figures show that the losses of the monolayer sample are slightly lower than those of the striated one. This can be caused by a somewhat higher self magnetic field component perpendicular to the substrate surface in the striated sample.

2.6 Comparison of transport ac losses with the losses in applied ac magnetic field and ways of reducing the losses:

Monolayer sample losses:
$Q_{self}(I=Ic)=0.01$ J/m/cycle
$Q_{field}(B=100mT)=0.13$ J/m/cycle
$Q_{field\ (extrapolated)}(B=1T)=1$ J/m/cycle

AC losses in a monolayer sample due to an applied magnetic field 1 T (peak) are substantially higher (by about 2 orders of magnitude) than transport ac losses. Subdivision of the monolayer sample into filaments (strips) with superconducting bridges (such as. samples C5 and C6) to increase the stability suppresses magnetization losses by a factor of about 2 (see Fig. 7). Such a sample would have a critical current I_c of about 100 A. A similar ac loss decrease can be expected for a striated sample with no superconducting bridges between the filaments (i.e. unstable), but with current leads soldered on its ends to enable the passage of the transport current. So the magnetization loss of such a "practical" sample at 1T (peak) would be about 0.5 J/m/cycle, which is still much higher than the transport ac loss at $I=I_c$ (0.01 J/m/cycle). A simultaneous application of the applied magnetic field in phase with transport current $I=I_c$ approximately doubles the in-field losses, so we obtain an estimated total loss $Q_{total}=2 \times Q_{field}(B=1T)=2 \times 0.5=1$ J/m/cycle.

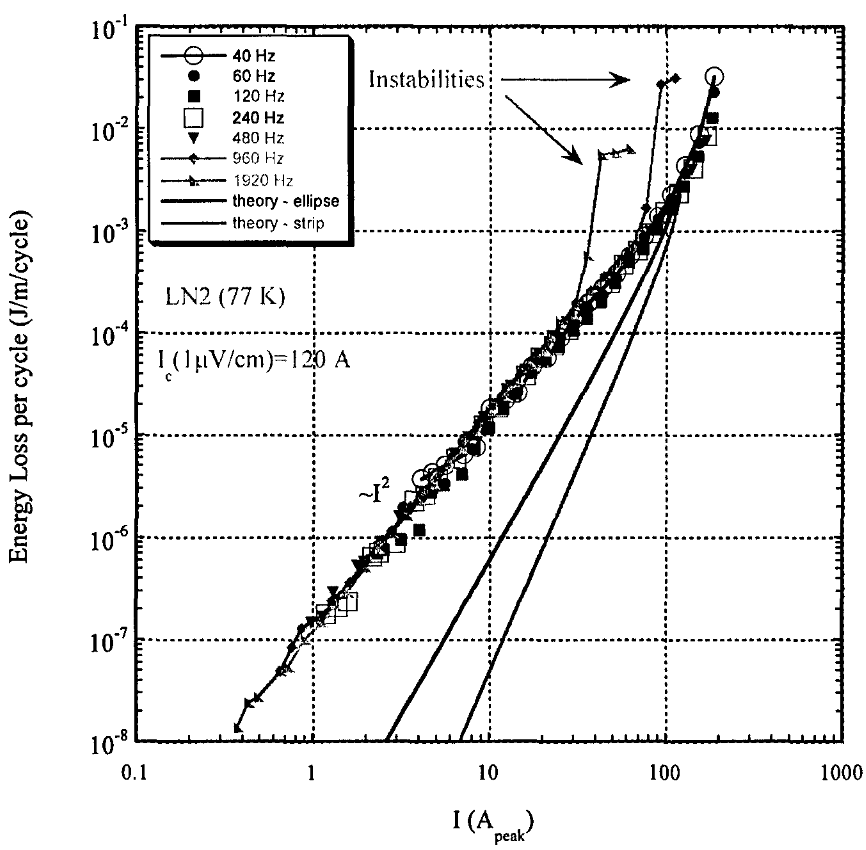

Fig. 17: Transport ac losses of Sample CM1 – filamentary part, $I_c(1\mu V/cm)=120$ A, measured in frequency range 40 Hz – 2 kHz.

However, this total loss is the so called "cold loss", which does not include the power needed to cool the sample. To calculate the real loss, i.e. the so-called "room temperature" loss, we need to

employ the second law of thermodynamics (the Carnot cycle). The minimum power requirement P_{min} to cool the sample heated by the total loss is then given by:

$$P_{\min} = Q_{total} \frac{T_{amb} - T_o}{T_o} \qquad 3$$

where Q_{total} (in watts) is the total power loss of the sample at operating temperature T_o and T_{amb} is the ambient temperature. For T_o=77 K, T_{amb}=300 K and a frequency of 50 Hz we obtain P_{min}=144.8 W/m.

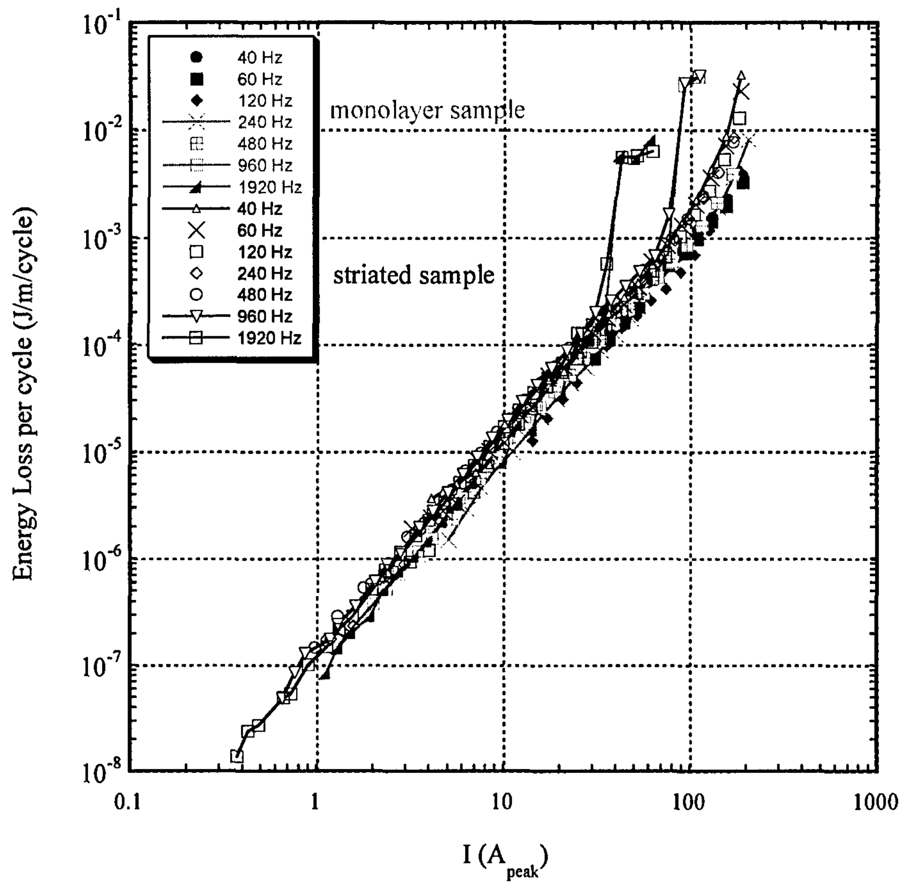

Fig. 18: Comparison of the transport ac losses of the monolayer and the filamentary sample.

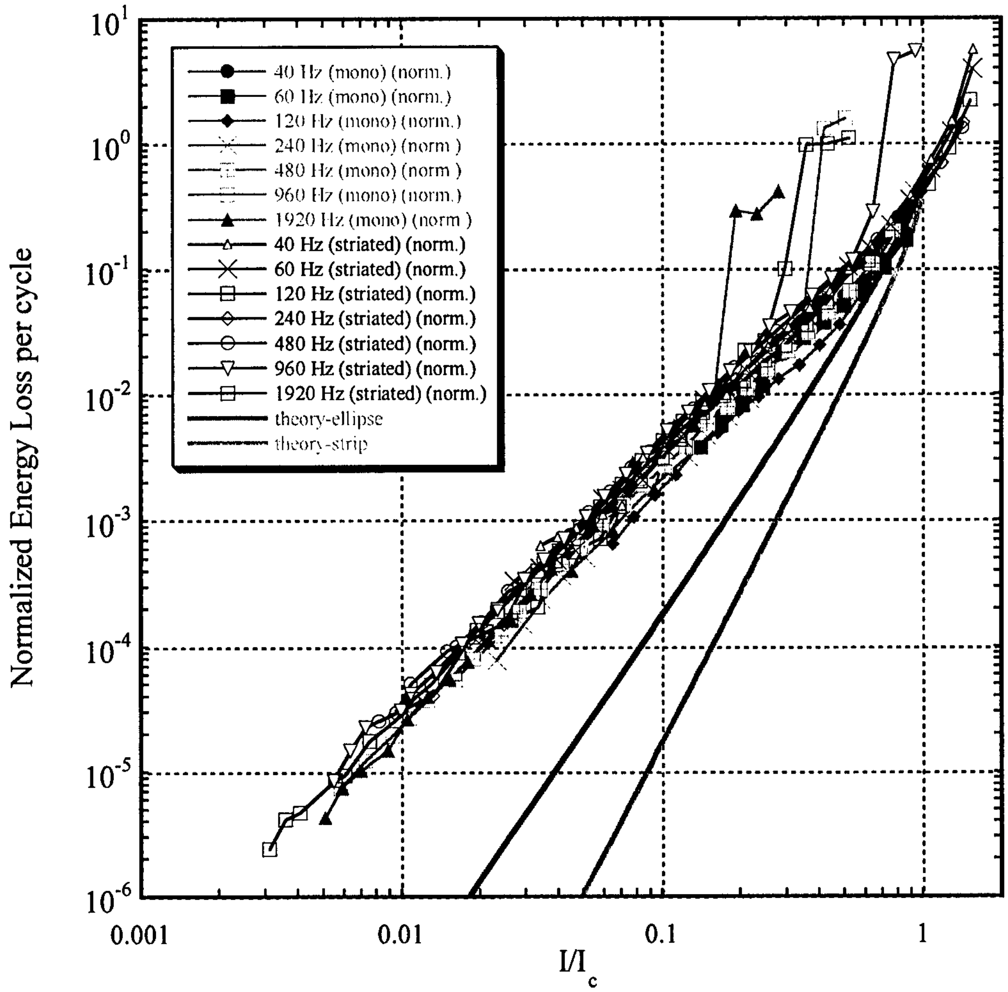

Fig. 19: Comparison of the normalized losses of the monolayer and the filamentary sample plotted against the normalized current.

If we propose to cool the sample by a cryocooler, then the required power of the cryocooler (i.e. the actual power) is given by

$$P_{act} = \frac{1}{\eta} P_{\min} \qquad 4$$

where η is the efficiency of the cryocooler cycle with respect to Carnot cycle. Most cryocoolers achieve $\eta \cong 0.2$ at 77 K. Then we obtain P_{act}=724 W/m.

If we compare the actual losses of our coated conductor with losses of an equivalent Cu round wire at 300 K, we obtain the following numbers. For Cu at 300 K we have the current density J=6A/mm^2 and the resistivity $\rho=1.69 \times 10^{-8}$ Ωm. So, to carry a current of 100A we need a Cu wire of 4.6 mm in diameter. Such a wire would have a loss of 63.85 W/m at 50 Hz in a field of 1 T (peak) applied in phase with the current 100 A (peak). This should be compared with actual loss of 724 W/m in our coated conductor. We see that actual losses of the coated conductor are about 1 order of magnitude higher than the losses of an equivalent Cu wire at room temperature. The only gain in using the coated conductor is the volume, because the ratio of the volumes of YBCO and Cu is $V_{YBCO}/V_{Cu}=6\times10^{-4}$ – i.e. the volume of Cu wire is more than 3 orders of magnitude higher than the volume of the coated conductor.

There exist a few ways to reduce ac losses in coated conductors. One of them is to use a cryocooler with a higher efficiency. Another one is to make the coated conductors work in an applied magnetic field parallel to their broad face. In such a way the in-field loss decrease would be proportional to their aspect ratio - in our case to $1cm/1\mu m = 10^4$. A transport current $I=I_c$ applied in-phase with the applied magnetic field roughly doubles the magnetization loss, so about 3 orders of magnitude of ac loss decrease could be achieved by this way. Parallel orientation of the coated conductors is not practical in most cases. In the perpendicular field orientation the only way of decreasing ac losses is to make a filamentary sample with twisted filaments. This method decreases in-field losses proportionally to the number of filaments, but it does not affect self-field losses. The point is that twisting decouples the filaments in applied field, but it does not decouple them in self-field. To reduce also the self-field losses the filaments must be either transposed or magnetically screened. This is very demanding from the point of view of technology, because it requires us to prepare at least 2 YBCO high quality films on top of each other.

Coated conductors do allow more varied ways of reducing the losses than multifilamentary conductors. One was suggested by Carr which is to twist the wire outside the rotor winding. This would mean a large twist pitch, but it is possible to put a high resistance layer between the substrate ad superconductor so that the skin depth is much larger than in a copper matrix. Ideally we would like to insulate each filament, but this would require every filament to be intact all the way along it length.

3. Future work

Transport AC losses of long lengths of the samples in the form of helical windings should be measured. Although the well defined different kinds of superconducting bridges between the filaments appear to be a viable way of producing filamentary samples with cryogenically stabilised filaments, new improved structures of the samples are required, namely double layer samples with patterned filaments connected at the edges, simulating a Rutherford cable. An apparatus enabling ac loss measurements in fields up to 2 T and at frequencies up to 400 Hz should be built.

4. Publications

1) M. Majoros, B. A. Glowacki, A. M. Campbell, G. A. Levin, P. N. Barnes, M. Polak, AC losses in striated YBCO coated conductors, Presented at 2004 Applied Superconductivity Conference, October 3-8, 2004, Jacksonville, Florida, USA (accepted for publication).
2) M. Majoros, B. A. Glowacki, A. M. Campbell, G. A. Levin, P. N. Barnes, Transport AC losses in striated YBCO coated conductors, to be presented at EUCAS'05 conference, Vienna